AIAA 81-0186R

Numerical Study of a Scramjet Engine Flowfield

J. Philip Drummond* and Elizabeth H. Weidner†
NASA Langley Research Center, Hampton, Va.

A computer program has been developed to analyze the turbulent reacting flowfield in a two-dimensional scramjet engine configuration. The program numerically solves the full two-dimensional Navier-Stokes and species equations in the engine inlet and combustor, allowing consideration of flow separation and possible inlet/combustor interactions. Results from the current program are presented that predict the flowfield for two inlet/combustor configurations, and comparisons of the program with experiment are given to allow assessment of the modeling that is employed.

Nomenclature

A,B = thermodynamic coefficients
c = local speed of sound or specific heat at constant pressure
e = total internal energy per unit volume
e_s = static internal energy
f = hydrogen mass fraction
H = total enthalpy
h = sensible static enthalpy
ℓ = mixing length
L_x = streamwise finite-difference operator
L_Y = transverse finite-difference operator
Le = Lewis number
p = pressure
Pr = Prandtl number
R = gas constant
Sc = Schmidt number
T = temperature
t = time
Δt = time increment
U_∞ = freestream velocity
u,v = streamwise and transverse velocity components
x,y = streamwise and transverse physical coordinates
α = species mass fraction
γ = ratio of specific heats
Γ = mass diffusion coefficient
δ = boundary-layer thickness
κ = heat-transfer coefficient
μ = total viscosity
ρ = density
σ = normal stress
τ = shear stress
ω = vorticity

Subscripts

c = chemical potential
i,j = x and y grid indices
k = chemical species index
p = chemical products
R = chemical reactants
x = in streamwise direction
y = in transverse direction

Superscript

0 = reference value at standard conditions

Introduction

INTEREST in the development of a supersonic combustion ramjet (scramjet) propulsion system for hypersonic cruise aircraft and missiles dates back a number of years.[1,2] A current program is underway at the NASA Langley Research Center to develop an airframe-integrated, hydrogen-fueled scramjet engine for hypersonic cruise applications in the atmosphere.[3,4] The engine is divided into several identical engine modules, one of which is shown in Fig. 1. The sidewall has been removed to reveal the engine internal structure. Each module consists of an inlet where the compression process begun by the vehicle undersurface is continued, fuel injection struts that complete the compression process and also provide locations for injection of gaseous hydrogen fuel, a combustor where the fuel and air are reacted, and a nozzle where the reacted mixture is expanded.

Fuel is introduced into the engine from the struts in both a parallel and transverse direction to the engine primary flow (Fig. 1). This approach tailors the injection to an optimum heat-release schedule in the engine over the flight Mach number range of interest. Transverse fuel injection promotes more rapid fuel/air mixing and is used whenever possible to promote reaction in the upstream portion of the combustor. When operating in the low Mach number range, however, too much perpendicular injection results in thermal choking of the engine. Therefore, the parallel injection mode predominates through the low Mach number range of operation at the expense of a somewhat longer reaction length.

Scramjet design requires a detailed understanding of the internal flowfield in the engine over a range of operating conditions. Computational tools can be particularly attractive for carrying out the needed studies, because analyses can be performed over a wide range of conditions relatively cheaply and without some of the difficulties associated with purely experimental approaches.[5] Computational analyses are not without their own set of problems, however. The flow in a scramjet engine is predominately supersonic, but there are regions of embedded subsonic flow in boundary layers along the strut and engine sidewalls, and in the combustor due to the chemical reaction taking place there. The subsonic regions can also separate as a result of shock/boundary-layer interactions and interaction of the primary flow with transverse fuel injectors in the combustor.[6] Finally, interactions between the inlet and combustor can also occur due to chemical reaction in the combustor, resulting in severe separation and choking of the engine. Computational analyses that attempt to model these phenomena must solve the full form of the equations of motion governing the flow of a compressible fluid.

Presented as Paper 81-0186 at the AIAA 19th Aerospace Sciences Meeting, St. Louis, Mo., Jan. 12-15, 1981; submitted Feb. 24, 1981; revision received Jan. 25, 1982.

*Aerospace Engineer, Computational Methods Branch, High-Speed Aerodynamics Division. Member AIAA.

†Mathematician, Hypersonic Propulsion Branch, High-Speed Aerodynamics Division.

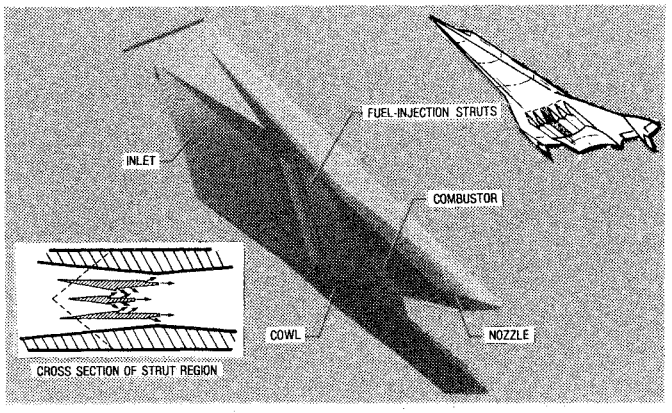

Fig. 1 Scramjet engine module.

The flow in the engine is also undergoing turbulent mixing and chemical reaction. Solution of the Reynolds stress equations might provide the turbulence field required by the governing equations, but such a solution is beyond the scope of available computer resources. Eddy viscosity models of turbulence have been developed primarily for boundary- or shear-layer flows, and only limited work has been done to extend these models to consider separated flows.[7] The chemical reaction of hydrogen fuel and air must also be considered in engine combustor analyses. Fortunately, a significant amount of work has been done for the hydrogen/air chemistry system.[8] Complete implementation of that work into an engine analysis tool requires, however, the solution of up to 12 species equations in addition to the equations of motion.[9] Solution of the full form of these species equations also appears prohibitive at the current time. Simple reaction models such as complete reaction or equilibrium chemistry are within the scope of the present work, but such models are completely justifiable only when reaction is mixing rather than kinetically controlled. A global finite-rate chemistry model, using a single or at most a few reaction paths, will likely offer the most promising model for describing hydrogen/air chemistry.

This paper discusses a computer program developed to study the flowfield in a two-dimensional scramjet engine model configuration. The current work represents an intermediate step toward development of a three-dimensional program to analyze actual scramjet engine flowfields. The governing equations are solved numerically using a well-known explicit predictor-corrector technique, turbulence is modeled using an algebraic eddy viscosity scheme, and chemistry is modeled using a hydrogen/air complete reaction model. Results from the current program are presented that predict the flowfield for two inlet/combustor configurations, and comparisons of the program with experiment are given to allow assessment of the modeling that is employed.

Analysis

Governing Equations

The flowfield in the scramjet engine model problem is governed by the complete Navier-Stokes equations and one or more additional transport equations describing the species present in the flow. Written in conservation law form for a simple hydrogen/air system in two-dimensional rectangular coordinates, these equations in the absence of body forces can be expressed as

$$\frac{\partial U}{\partial t}+\frac{\partial F}{\partial x}+\frac{\partial G}{\partial y}=0 \tag{1}$$

where

$$U=\begin{Bmatrix}\rho\\ \rho u\\ \rho v\\ e\\ \rho f\end{Bmatrix} \tag{2}$$

$$F=\begin{Bmatrix}\rho u\\ \rho u^2+\sigma_x\\ \rho uv+\tau_{xy}\\ (e+\sigma_x)u+\tau_{yx}v+q_x\\ \rho uf+\dot{m}_x\end{Bmatrix} \tag{3}$$

$$G=\begin{Bmatrix}\rho v\\ \rho uv+\tau_{yx}\\ \rho v^2+\sigma_y\\ (e+\sigma_y)v+\tau_{xy}u+q_y\\ \rho vf+\dot{m}_y\end{Bmatrix} \tag{4}$$

and

$$\sigma_x=p-\lambda\left(\frac{\partial u}{\partial x}+\frac{\partial v}{\partial y}\right)-2\mu\frac{\partial u}{\partial x} \tag{5}$$

$$\tau_{xy}=\tau_{yx}=-\mu\left(\frac{\partial u}{\partial y}+\frac{\partial v}{\partial x}\right) \tag{6}$$

$$\sigma_y=p-\lambda\left(\frac{\partial u}{\partial x}+\frac{\partial v}{\partial y}\right)-2\mu\frac{\partial v}{\partial y} \tag{7}$$

$$\lambda=-\frac{2}{3}\mu \tag{8}$$

$$\kappa=\gamma u/Pr \tag{9}$$

$$\Gamma=\mu/Sc=\mu/Pr \qquad (Le=1) \tag{10}$$

$$\mu=\mu_{\text{laminar}}+\mu_{\text{turbulent}} \tag{11}$$

$$q_x=-\kappa\frac{\partial e_s}{\partial x} \tag{12}$$

$$q_y=-\kappa\frac{\partial e_s}{\partial y} \tag{13}$$

$$\dot{m}_x=-\Gamma\frac{\partial f}{\partial x} \tag{14}$$

$$\dot{m}_y=-\Gamma\frac{\partial f}{\partial y} \tag{15}$$

$$e_s=\int_0^T(c-R)\,dT=\bar{c}T \tag{16}$$

The specific heat is a function of the local temperature and species concentrations. The pressure is calculated from the equation of state for an ideal gas and the laminar viscosity is calculated from Sutherland's law. The turbulent viscosity is calculated from the algebraic eddy viscosity model described in Ref. 7. This particular scheme was developed to empirically

model separated flow by using the vorticity rather than the boundary-layer thickness to characterize the scale of turbulence. The boundary-layer thickness is difficult to define in a separated flow.

To adequately resolve large flowfield gradients, the physical coordinate grid must be very fine near walls and major flowfield disturbances. Well away from these regions where gradients are small, a coarser physical grid can be used for computational efficiency while still adequately resolving the flowfield. A transformation of the independent variables is therefore needed to transform the nonuniform grid in the physical domain to a uniform grid in the computational domain. Equations (1-15) are transformed from the physical domain to the computational domain using the transformations of Roberts[10] and Holst.[11] Details for applying these transformations are given in Ref. 12.

Solution of Governing Equations

The time-split finite-difference technique of MacCormack[13] is used to integrate the governing equations until a steady-state solution is reached. If a solution to Eq. (1) is known at some time $t=n\Delta t$, the solution at the next time step, $t=(n+1)\Delta t$ can be calculated from

$$U_{i,j}^{n+1}=L(\Delta t)\,U_{i,j}^{n} \tag{17}$$

for each node point (i,j) in a finite-difference grid network within the boundaries of the computational domain. The finite-difference operator L is split into two one-dimensional difference operators $L_x(\Delta t)$ and $L_y(\Delta t)$. Each split operator consists of a predictor and corrector integration step as described in Ref. 13. The one-dimensional operators are combined to form a two-dimensional operator through the symmetric operator sequence[13]

$$L(\Delta t)=L_y(\Delta t/2)\,L_x(\Delta t)\,L_y(\Delta t/2) \tag{18}$$

One pass through Eq. (18) advances the finite-difference form of Eq. (1) through one time step, Δt. Oscillations that develop in the neighborhood of strong shocks and expansions during the integration process are smoothed using a modified form[6] of the MacCormack fourth-order pressure damping scheme.[13]

Boundary Conditions

No slip boundary conditions were used along walls to specify the velocity components. The wall is assumed adiabatic, so that the normal derivative of temperature must vanish. The normal derivative of the total hydrogen mass fraction is also required to vanish along the wall to satisfy the noncatalytic wall boundary condition. The pressure is determined from the normal momentum equation[13] and the density is calculated from the ideal gas law.

To prescribe boundary conditions along a symmetry plane, the normal derivative of the u velocity is also required to vanish. The inflow and hydrogen injection boundaries are predominately supersonic. Therefore, boundary conditions along the inflow plane are normally specified by holding the velocities, temperature, pressure, and mass fraction fixed at their initial values and then calculating the density and total internal energy. Along the outflow plane, all dependent variables are found by zeroth order or linear extrapolation from upstream values, other than the density and total internal energy which are again calculated. At a hydrogen fuel injector, boundary conditions are specified by fixing all dependent variables at their initial values consistent with the required physical behavior of the jet.

Chemistry Model

The chemical reaction of hydrogen fuel and air is modeled in the present work using a complete reaction model. This model assumes that instantaneous reaction occurs at any point where both fuel and air are present. The extent of reaction is determined by the stoichiometric limit of the hydrogen/air reaction, i.e., the amount of hydrogen present determines the extent of reaction with a fuel lean condition and the amount of oxygen present determines the extent of reaction with a fuel-rich condition. No reaction is allowed when the fraction of hydrogen in air is less than 4% by volume.

Once the new composition is determined at a given computational node after reaction, the total enthalpy of the products, which must equal the total enthalpy of the reactants, is given by

$$H_p=\sum_k\int_{T^0}^{T}\alpha_k c_k\,\mathrm{d}T+\frac{u^2+v^2}{2}+H_c \tag{19}$$

where

$$H_c=[\alpha_{H_2}H_{H_2}^0+\alpha_{H_2O}H_{H_2O}^0+\alpha_{N_2}H_{N_2}^0+\alpha_{O_2}H_{O_2}^0]_{T=T^0}$$

Over the range of temperatures being considered in this work, it is reasonable to assume that the specific heat for each species being considered is a linear function of temperature, i.e.,

$$c_k=A_kT+B_k \tag{20}$$

Substituting Eq. (20) into Eq. (19) and integrating gives

$$H_R=\tfrac{1}{2}\bar{A}_pT^2+\bar{B}_pT-\bar{h}_p^0+\frac{u^2+v^2}{2}+(H_c)_{T^0}$$

where

$$\bar{h}_p^0=\tfrac{1}{2}\bar{A}_pT^{0^2}+\bar{B}_pT^0$$

$$\bar{A}_p=\sum_k\alpha_kA_k$$

$$\bar{B}_p=\sum_k\alpha_kB_k$$

Solving for T and selecting only the positive root yields the temperature after reaction

$$T=(-\bar{B}_p+\sqrt{\bar{B}_p^2+2\bar{A}_pH_T})/\bar{A}_p \tag{21}$$

where

$$H_T=H_R+\bar{h}_p^0-\frac{u^2+v^2}{2}-(H_c)_{T^0}$$

The chemistry model is applied at the end of each computational time step. Once the new composition (hydrogen, oxygen, nitrogen, and water) is known, a new temperature is determined at each computational node and the gas mixture properties are recomputed. The calculation then proceeds to the next time step.

Results

Analyses have been carried out for two cases to be presented. The first case considers the sonic slot injection of gaseous hydrogen from a flat plate at zero angle of attack into a supersonic crossflow. Comparisons of the program results with experimental data from the case are described to allow assessment of the modeling that is employed in the analysis when considering transverse fuel injection into a supersonic flow. The second case involves the analysis of a complete two-dimensional scramjet engine. Two fuel injector configurations are considered in the analysis and engine performance is predicted for each configuration.

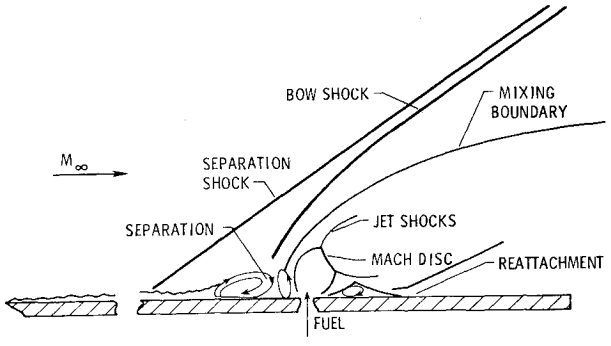

Fig. 2a Schematic of transverse fuel injector flowfield in Thayer experiment.

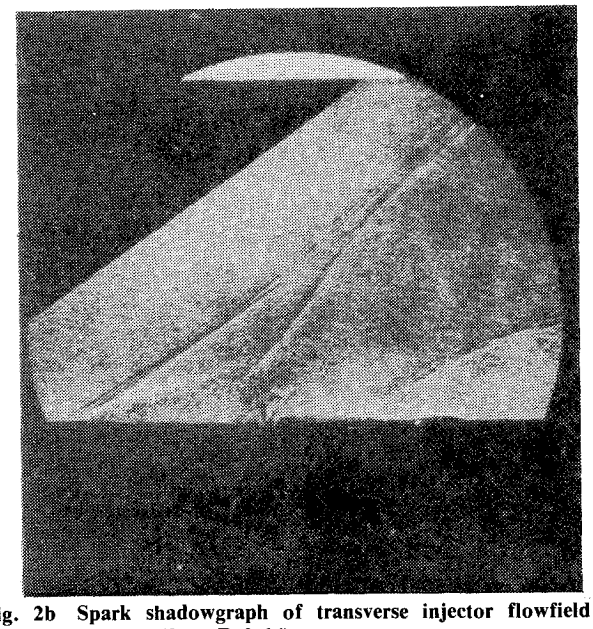

Fig. 2b Spark shadowgraph of transverse injector flowfield in Thayer experiment (from Ref. 14).

The first test case provided a comparison of the computer program with nonreacting experimental data; the configuration for this case is shown in Fig. 2.[14] Gaseous hydrogen was injected from a choked 0.02 cm slot on a flat plate at zero angle of attack into a supersonic air cross stream. The slot was 5.08 cm long and located 25.6 cm from the leading edge of the plate. The flowfield with this slot length was verified in Ref. 14 to be nearly two-dimensional within the region of interest. A turbulent boundary layer was produced by tripping the flow 2.54 cm from the plate leading edge. This experiment represents the only case known to the authors in which species measurements were made to determine hydrogen concentration away from the slot.

The case was by no means ideal for verification of the present computer program, however. The jet-to-freestream pressure ratio was significantly higher than ratios encountered in scramjet design (a static jet-to-freestream pressure ratio of 43 as compared to pressure ratios of 2-15 in the engine) and the slot width was quite narrow. These two conditions combined to produce extremely large gradients near the slot, complicating numerical analysis of the problem. It should be noted that large flowfield gradients also complicate the accurate acquisition of data near the fuel injector. In addition, only conditions along the wall upstream of the slot were measured. No surveys were available away from the plate.

The conditions of the hydrogen at the slot exit were $M=1.0$, $T=243$ K, and $p=0.728$ MPa. The conditions of the air just upstream of the leading edge of the flat plate were $M=2.5$, $T=130$ K, and $p=0.0169$ MPa.

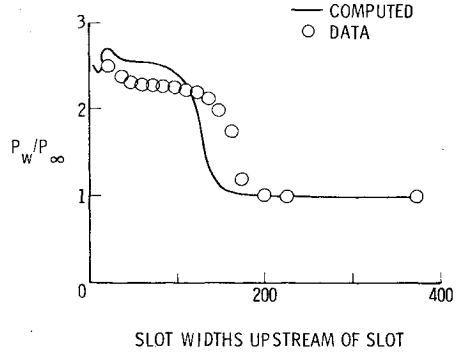

Fig. 3 Comparison of experimental (Thayer) and computed wall pressures.

The overall plate length made it computationally impracticable to begin the calculation ahead of the leading edge. Therefore, a 10×10 cm domain was chosen and centered about the hydrogen injector. The lower boundary was made coincident with the plate and the upper boundary was placed well into the freestream. Initial conditions were specified by assuming the presence of a turbulent boundary layer on the plate with the boundary-layer thickness defined by[15]

$$\delta = 0.37x(\rho U_\infty x/\mu_\ell)^{-0.2}$$

The streamwise velocity in the boundary layer was then defined using the one-seventh power law distribution[15]

$$u/U_\infty = (y/\delta)^{1/7}$$

All remaining dependent variables were then initialized at interior points by enforcing conservation principles. Values at the inflow station were initially calculated by linear extrapolation from downstream; however, once these values reached steady state, they were held fixed for the remainder of the integration such that the flowfield could be studied in a finite-computational space.

The physical domain was spanned by a finite-difference grid with 81 nodes in the streamwise direction along the plate and 30 nodes normal to the plate. The grid was compressed in both a transverse direction near the wall and in a streamwise direction near the injector such that at least eight nodes transversely spanned the turbulent boundary layer and three nodes longitudinally spanned the fuel injector at the plate interface. Other computations were also made with a longer streamwise domain to examine the dependence of the solution on the location of the inflow and outflow boundaries. Additionally, other grid distributions were considered about the fuel injector. None of those changes affected the solution within 400 slot widths of the injector, which was the region of interest for this study.

Comparison of the program results with Thayer's experimental data is given in Fig. 3. The figure shows values of the static wall pressure as a function of slot widths along the plate upstream of the injector. The calculated wall pressure agrees reasonably well with the data. The wall pressure rise is predicted to begin approximately 155 slot widths upstream of the injector, whereas the data indicate the rise begins about 175 slot widths ahead of the injector. The pressure plateau values predicted by the program also agree reasonably well with the data, the calculated values being approximately 9% higher than the experimental values. The slight oscillation in the wall pressure very near the slot is a numerical preshock oscillation associated with the jet shock. Slightly further downstream, the pressure rises to 43 times the freestream pressure. A comparison of the calculated and experimental values of hydrogen mass fraction along the wall was also made and detailed results are given in Ref. 12.

Results for the first case indicate fair agreement between wall pressures predicted by the program and measured wall pressure data. The location of the separation ahead of the injector was underpredicted somewhat by the program. This difference could have been caused by the turbulence model or by failure to properly resolve the boundary layer along the plate, resulting in an underestimation of feedback effects through the subsonic portion of the boundary layer. To examine these differences further, other comparisons of the program with experiment, including both wall and cross-stream survey data, have been made. These comparisons are documented in Ref. 16.

The second case considers the turbulent, reacting flowfield in a two-dimensional scramjet engine model problem. The configuration for the problem is described in Fig. 4. The engine module is 78 cm long and 15 cm high at the inlet leading edge. The fuel injection strut is 25.8 cm long and is centered about the module cross-sectional minimum located 37.8 cm from the inlet leading edge. The engine sidewall angles and strut half-angles are 7.1 deg. This geometry is a two-dimensional projection of an actual scramjet engine design. Flow enters the inlet at $M=5.03$, $T=335$ K, and $p=3546$ Pa. Hydrogen is injected transverse to the main flow from the single fuel injection strut and the engine sidewalls at $M=1.05$, $T=246$ K, and $p=254{,}824$ Pa. This injection results in fuel equivalence ratio of one. Following inlet compression, the hydrogen jet-to-air static pressure ratio is about 2.5. The four transverse injectors (Fig. 4) are located 6 cm downstream of the engine cross-sectional minimum and are each 0.1 cm wide.

The physical domain for this problem was chosen to begin 10 cm upstream of the inlet leading edge and to end at the combustor outlet. The domain was bounded transversely by the lower engine sidewall and the engine centerline. The flowfield between the centerline and the upper engine sidewall is symmetric with the flow below the centerline; those results were inferred by symmetry. The physical domain was spanned by a grid with 87 nodes in the streamwise direction and 30 nodes in the transverse direction.

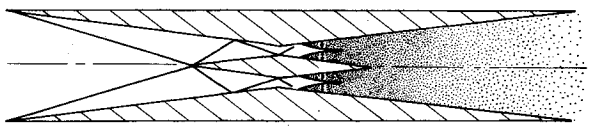

Fig. 4 Schematic of scramjet engine problem with expected shock structure and injector locations.

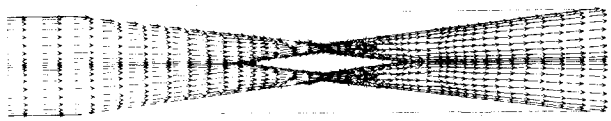

Fig. 5 Computed velocity vector field in engine.

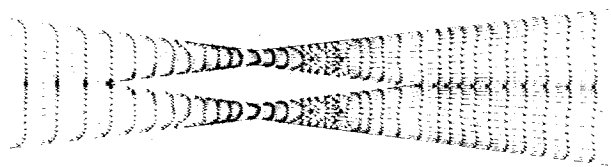

Fig. 6 Magnified velocity vector field in engine.

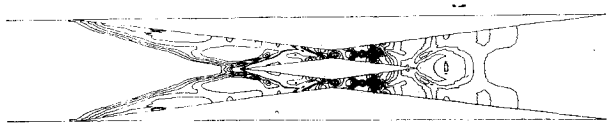

Fig. 7 Computed static pressure contours in engine.

Results for the engine case are summarized in Figs. 5-10. Figure 5 shows the velocity vector field in the engine. Details of the flow near the minimum can be seen in the magnified vector plot presented in Fig. 6. The air entering the inlet is turned rather abruptly by shocks from the inlet leading edges. Shocks are indicated by a coalescence of pressure contour lines (Fig. 7). These shocks strike near the strut leading edge and coalesce with shocks produced by the strut. The resulting shocks then have sufficient strength to separate the boundary layer when they reach the engine sidewalls, as indicated by a reversal of the velocity vectors to an upstream direction. Induced shocks then result from the separation.

The transverse hydrogen fuel injectors located downstream of the minimum can also be seen in the figures along with their associated flow separations leading and trailing the injectors. The flow becomes subsonic near the fuel injectors due to both the main flow blockage by the injectors and the heat release from chemical reaction. Some reaction takes place in the separated regions ahead of the injectors; significant reaction occurs downstream of the injectors.

The effect of chemical reaction on the static temperature field can be seen in Fig. 8. Contours are plotted for temperatures of 400, 600, 1000, 1400, 1800, 2200, and 2600 K. Maximum temperatures are reached in the separated regions just ahead of the injectors and at the edge of the hydrogen/air mixing layer just downstream of the injectors. It is at these locations that the highest degree of reaction occurs. For the conditions shown here, the injectors are not of sufficient strength to penetrate across the flow at the point of injection, and the opposing mixing layers do not meet until approximately 11 cm downstream of the injectors. Reaction occurs across the entire flowfield beyond this point, although the highest degree of reaction still occurs in the interior of the mixing layers. Mixing and reaction could be improved by moving the injectors further upstream toward the minimum to allow more combustor length for mixing or by raising the injection pressure (while narrowing the slot width so as to preserve the same equivalence ratio) to improve fuel penetration into the air crossflow.

Figure 9 describes the total hydrogen mass fraction distribution, i.e., gaseous hydrogen or hydrogen in water in the combustor. Total hydrogen is computationally conserved to 1.9% and total mass, i.e., total hydrogen and air, is conserved to 0.2% in the combustor. Contours are plotted for 0.1, 1, 10, 20, and 40% by mass of hydrogen. This distribution provides a good indication of fuel/air mixing. The highest concentrations of hydrogen lie closest to the strut and engine sidewalls, but concentrations of around 1% hydrogen do penetrate across the flow downstream of the

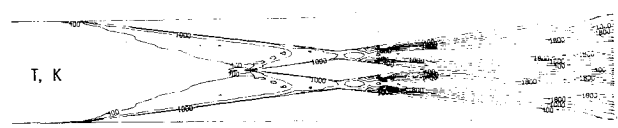

Fig. 8 Computed static temperature contours in engine.

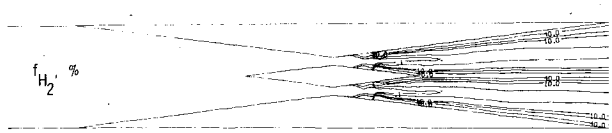

Fig. 9 Computed total hydrogen contours in engine.

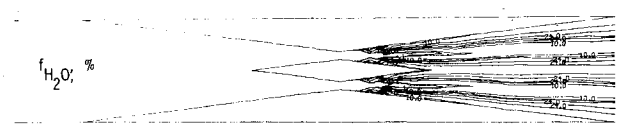

Fig. 10 Computed water contours in engine.

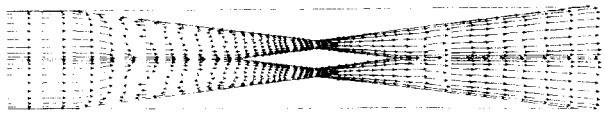

Fig. 11 Computed velocity vector field in engine with choked flow.

injectors. These results indicate a need to relocate or reconfigure the injectors to improve fuel penetration and mixing. Ideally, the fuel should be well mixed with air throughout the flowfield downstream of the injectors. The program allows the degree of mixing to be evaluated over a range of configurations so that the injector design and location can be optimized. Figure 10 shows the water mass fraction distribution in the combustor for contours of 0.1, 1, 10, 20, and 24%. The results again agree with the previous figures in that the maximum concentration of water lies midway through the fuel/air mixing layers where the degree of reaction is the highest and the temperatures peak. Values of water concentration midway across cross-sectional planes in the combustor are still quite low, however, again emphasizing the need to improve fuel penetration and mixing.

To attempt improvement of fuel/air mixing, the injectors were relocated 4.7 cm upstream of the previous injector location (or 1.3 cm downstream of the engine cross-sectional minimum). The injector pressure was also reduced by a factor of two resulting in an equivalence ratio of 0.5. No other changes in geometry or flow conditions were made from the previous case. Results for this case are given in Fig. 11. Figure 11 provides a velocity vector field plot of the engine flowfield. Note the large regions of separated flow in the inlet that persist nearly to the leading edge. The separation results from choking at the engine minimum that produces a very adverse pressure gradient along the engine sidewalls. The fuel injector location for this engine geometry would not be acceptable. The calculation was terminated once the massive separations and a severe mass imbalance formed. The program could be used to find the resulting flowfield after the engine choked by redefining the physical domain and boundary conditions. Such information is not that helpful, however, once it has been determined that a particular engine configuration is not useful. To investigate the source of the choking problem, the above calculation was repeated without chemical reaction. The calculation then proceeded normally with mass conserved and without the appearance of any significant separation. Therefore, it was concluded that thermal choking was produced by chemical reaction and subsequent heat release near the injectors.

The preceding two-dimensional engine calculations have been performed to show the potential for analytically predicting scramjet performance information over a range of conditions. The present computer program has been used to successfully calculate details of the turbulent reacting flowfield in a scramjet, and has provided information needed to actually design an engine. All calculations were carried out on a Control Data CYBER-203 vector processing computer. Engine solutions required up to 2887 s on the 87×30 grid. Further extension of the program to three dimensions, along with the addition of improved chemistry and turbulence models, will be necessary before actual three-dimensional engine configurations can be considered. The successful analysis of a two-dimensional scramjet engine model problem indicates, however, that such an extension is feasible. Computer growth will likely be the pacing item for a complete engine analysis.

Conclusion

A computer program has been developed to analyze the turbulent reacting flowfield in a two-dimensional scramjet engine configuration. The program numerically solves the full two-dimensional Navier-Stokes and species equations in the engine inlet and combustor, allowing consideration of flow separation and possible inlet/combustor interactions. A transverse hydrogen fuel injector problem for which experimental data were available was analyzed to allow assessment of the modeling used in the program. The comparison yielded fair agreement between experimental and computational wall pressures.

Two-dimensional, reacting, scramjet engine flowfields were also analyzed by the program. Results were presented to demonstrate the potential for providing useful analysis and design information with an analytical engine analysis tool. These results showed for the engine case considered in this paper that there was insufficient penetration of hydrogen to allow good fuel/air mixing. This effect reduced the overall level of reaction in the upstream portion of the combustor yielding reduced engine performance. An attempt was made to improve penetration by moving the injectors further upstream toward the engine cross-sectional minimum. The program then predicted that the engine would thermally choke due to severe disturbances produced by the fuel injectors and chemical reaction near the engine minimum. The analyses carried out for this case provided examples of two extremes that would be encountered during parametric studies of candidate scramjet engine configurations.

References

[1] Henry, J. R. and Beach, H. L., "Hypersonic Air Breathing Propulsion Systems," Paper 8, NASA SP-292, Nov. 1971.

[2] Waltrup, P. J., Anderson, G. Y., and Stull, F. D., "Supersonic Combustion Ramjet (Scramjet) Engine Development in the United States," Paper presented at 3rd International Symposium on Air Breathing Engines, Munich, FRG, March 1976.

[3] Jones, R. A. and Huber, P. W., "Toward Scramjet Aircraft," *Astronautics and Aeronautics,* Vol. 16, Feb. 1978, pp. 38-48.

[4] Hearth, D. P. and Preyss, A. E., "Hypersonic Technology—Approach to an Expanded Program," *Astronautics and Aeronautics,* Vol. 14, Dec. 1976, pp. 20-37.

[5] Drummond, J. P., Rogers, R. C., and Evans, J. S., "Combustor Modelling for Scramjet Engines," Paper 10, AGARD-CP-275, Oct. 1979.

[6] Drummond, J. P., "Numerical Investigation of the Perpendicular Injector Flow Field in a Hydrogen Fueled Scramjet," AIAA Paper 79-1482, July 1979.

[7] Baldwin, B. S. and Lomax, H., "Thin Layer Approximation and Algebraic Model for Separated Turbulent Flows," AIAA Paper 78-257, Jan. 1978.

[8] Bahn, G. S., "Calculations on the Autoignition of Mixtures of Hydrogen and Air," NASA CR-112067, April 1972.

[9] Evans, J. S. and Schexnayder, C. J., "Critical Influence of Finite Rate Chemistry and Unmixedness on Ignition and Combination of Supersonic H_2-Air Stream," AIAA Paper 79-0355, Jan. 1979.

[10] Roberts, G. D., "Computational Meshes for Boundary Layer Problems," *Lecture Notes in Physics,* Springer-Verlag, New York, 1971, pp. 171-177.

[11] Holst, T. L., "Numerical Solution of Axisymmetric Boattail Fields with Plume Simulators," AIAA Paper 77-224, Jan. 1977.

[12] Drummond, J. P. and Weidner, E. H., "Numerical Study of a Scramjet Engine Flow Field," AIAA Paper 81-0186, Jan. 1981.

[13] MacCormack, R. W. and Baldwin, B. S., "A Numerical Method for Solving the Navier-Stokes Equations with Application to Shock-Boundary Layer Interactions," AIAA Paper 75-1, Jan. 1975.

[14] Thayer, W. J., "The Two-Dimensional Separated Flow Region Upstream of Inert and Chemically Reactive Transverse Jets," Ph.D. Thesis, Dept. of Mechanical Engineering, University of Washington, Seattle, 1971.

[15] Schlicting, H., *Boundary Layer Theory,* McGraw Hill Book Co., New York, 1968.

[16] Weidner, E. H. and Drummond, J. P., "A Parametric Study of Staged Fuel Injector Configurations for Scramjet Applications," AIAA Paper 81-1468, July 1981.